Non-Obtrusive Detection of Concealed Metallic Objects Using Commodity WiFi Radios

Asif Hanif, Muhammad Saad Chughtai, Abuzar Ahmad Qureshi, Abdullah Aleem,
Farasat Munir, Muhammad Tahir, and Momin Uppal
Department of Electrical Engineering, Lahore University of Management Science, Lahore, Pakistan.
Emails: {asif.hanif, 18100094, 18100075, 18100135, farasat.munir, tahir, momin.uppal}@lums.edu.pk

***Abstract*—In light of increasing interest in detection of concealed metallic weapons, there is a great need to have robust and non-obtrusive metal detection systems with large coverage areas. Conventional systems based on electromagnetic induction or X-rays are effective, but have small coverage areas in addition to requiring costly infrastructure. In this paper, we explore the use of ubiquitously present WiFi signals for non-obtrusive detection of concealed metal objects. For the purpose, we build a prototype system consisting of a single-antenna commodity WiFi radio as a transmitter, and two multi-antenna radios as receivers placed in an indoor environment of approximately 42 ft $\times$ 39 ft. We conduct extensive experiments with subjects walking through the setup with (or without) a sheet of metal placed around their chests. We use the channel state-information collected from the receivers to train a deep convolutional neural network, and find that the proposed system can differentiate between the metal and non-metal cases with an average accuracy of 86.44%.**

***Index Terms*—WiFi Sensing, Metal Detection, Deep Neural Network, Weapon Detection, CSI**

I. Introduction

Metal detectors have become essential for ensuring security at airports, military headquarters, courthouses, prisons, schools, parks, and even offices. Additional applications include geophysical prospecting, land-mine detection, treasure hunting, detection of metallic objects/pipes/wires buried underground or inside walls [1], and detection of metal-contaminated food before packaging [2].

Metal detectors usually exist in the form of hand-held devices or walk-through gates, and are mostly based on electromagnetic induction. Another widely used technique for metal detection is X-ray imaging. Since, electromagnetic radiations cannot pass through metallic objects, illumination by X-rays shows a metallic object as a deep shadow in the reflected energy image [3]. However, since exposure to X-rays can have adverse effects on human health, the use of X-rays in crowded areas is not a good option for metal detection. Another emerging alternative is the use of near-field imaging methods based on non-ionizing radiation including active and passive sensing techniques [4]. Passive imaging techniques such as infrared and passive millimeter wave (mmW) imaging suffer from low resolution and higher noise effects which lead to blurry imaging [5]. On the other hand, active mmW imaging is attractive due to its high quality and high resolution [6]. Although these conventional metal detection systems have proved to be effective, they have a major drawback. They usually have limited coverage and therefore require subjects to pass through them one at a time, creating bottlenecks at crowded locations. In addition, majority of these systems require installation of costly specialized infrastructure.

In light of the drawbacks mentioned above, there is a need for expedited security screenings using low-cost non-obtrusive metal detection systems that have wide coverage areas. In this paper, we explore the use of an unconventional approach that utilizes ubiquitously present WiFi radio signals for low-cost non-obtrusive detection of concealed metal objects on a person. As unconventional as it may sound, the utility of these radio signals for metal detection is not far-fetched. Indeed, radio signals reflect differently from a metallic object than they do from non-metallic material. As a result, the premise of our proposed solution is that the presence of a metallic object in the path of radio signals creates specific patterns in received channel state information (CSI); patterns that could then be identified for effective classification. Relying on this premise, we build a prototype system that illuminates targets with an off-the-shelf Intel 5300 WiFi radio connected to a directional horn-antenna. As receivers, the system uses the same off-the-shelf multi-antenna radios placed nearby as shown in Fig. 1. To the best of our knowledge, the only work in existing literature to have dealt with metal detection using WiFi is [7]. However, the system in [7] requires that the subject remain stationary while being "scanned" - the robustness of the system while the subject is moving was not tested. As opposed to [7], our proposed framework is based on the vision in which no "cooperation" from the target is expected. More precisely, using WiFi radios, we attempt metal detection on a person who moves through the illumination area at regular walking speeds. For increasing the likelihood of accurate detection despite the diffuse reflections and randomly varying artifacts caused by target motion, we rely on signal diversity by employing two multi-antenna receivers. We conduct extensive experiments with subjects walking through the illumination area either without or with a metal sheet placed near their chests. Using the corresponding CSI collected from the two receiving nodes as training data, we use a deep convolutional neural network (CNN) for differentiating between the two cases. Using a 10-fold cross validation over data from 459 experiments and four different subjects, the average accuracy of the proposed approach is found to be 86.44%. While there

978-1-5386-4727-1/18/$31.00 ©2018 IEEE

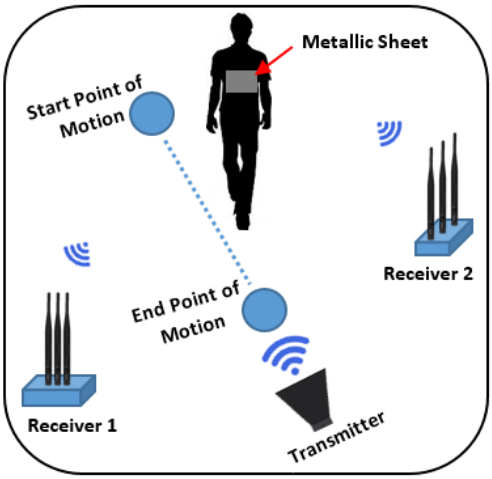

Fig. 1. An illustration of the proposed system

remains several aspects that need to be explored further, the preliminary experimental results we report in this paper point to the promise of WiFi radios as a means towards full-fledged low-cost systems for non-obtrusive detection of concealed metal objects.

The remainder of the paper is organized as follows. In Section II, we provide a description of the proposed system for metal detection using WiFi radios. In Section III, we discuss, through our experimental observations, how the presence of a metal object in the illumination area affects the receive CSI as well as details of the classification algorithm we utilize when the target is in motion. Section IV presents the details of our experimental setup, as well as the classification results, while Section V concludes the paper.

II. Proposed System for Concealed Metal Detection

The main idea of the proposed framework is to detect the concealed metallic object on a human subject by recording and processing the changes in CSI amplitude. Fig. 1 illustrates the proposed setup with one transmitting node illuminating a spatial region by directing its energy in a narrow beam using a directional horn antenna. As a subject walks through this region, two receiving nodes[1], each equipped with three omnidirectional antennas, collect the reflected energy from the person's body. The received signal is used to extract CSI, with a CNN used for classification purposes. In the following, we provide an overview of what the CSI corresponds to in the context of our system, followed by a description of how it is pre-processed before being input to a CNN.

A. CSI and Metal Detection

WiFi (IEEE 802.11 a/g/n) utilizes orthogonal frequency division multiplexing (OFDM) with data transmitted over multiple sub-bands to combat frequency selective fading. Loosely speaking, the CSI captures the channel characteristics of the individual sub-bands in the form of complex numbers. More precisely, if $\underline{\mathbf{x}}$ is a length-M vector of transmitted symbols (one for each sub-band), the received vector $\underline{\mathbf{y}}$ over the M sub-bands can be written as

$$\underline{\mathbf{y}} = \mathbf{H}\underline{\mathbf{x}} + \underline{\mathbf{n}}, \tag{1}$$

where $\underline{\mathbf{n}}$ is additive White Gaussian noise vector and $\mathbf{H}$ is a diagonal matrix with the element-i on the diagonal representing the complex channel response associated with sub-band-i. This element-i is given as

$$\mathbf{H}_i = \sum_{k=1}^{K} r_k e^{-j2\pi F_i \tau_k} = |\mathbf{H}_i| e^{j\theta_i}, \tag{2}$$

where K represents total number of multipath components, F_i is the sub-carrier frequency, r_k is the attenuation and τ_k is the propagation delay of k-th path respectively; $|\mathbf{H}_i|$ and θ_i correspond to the magnitude and phase of H_i, respectively. This fine grained CSI information (estimated through training symbols) corresponding to the wireless channel is now accessible in many commercially available off-the-shelf WiFi devices. The basic premise behind detecting concealed metallic objects using WiFi radios is that the presence of metal introduces changes in the received signal which can then be detected and differentiated from non-metal cases. In order to detect the changes in received signal, one can either rely on the Received Signal Strength (RSS) or the CSI. RSS has severe variations especially during target motion and Non-Line-Of-Sight (NLOS) conditions. On the other hand, CSI information has been shown to be a more stable and accurate representation of the wireless channel especially in the case of NLOS conditions with small scale fading components [8]. As a result, we utilize the CSI information for detecting changes in received signal properties.

Out of 56 data subcarriers for data transmission over a 20 MHz bandwidth channel used by WiFi radios, we can access 30 subcarrier CSI information using firmware modifications [9]. Extracted CSI contains the information of $\mathbf{H}_i$ at the symbol rate for 30 subcarriers. Over the years, researchers have exploited the rich contextual information available in the CSI for a number of applications such as human activity recognition [10], vital signs monitoring [11], gesture recognition [12] , keyboard stroke recognition [13], gait recognition [14], intrusion detection [15] and human identity detection [16]. For our work, we focus on the use of CSI magnitudes $|\mathbf{H}_i|$ for the detection of concealed metallic object on a subject.

B. CSI Preprocessing

Since each one of the two receiving nodes is equipped with three antennas, there are six receive antennas in total. The CSI stream corresponding to each antenna was pre-processed to extract information corresponding to target motion only. After removing the initial and final transients, a stream of 5000 epochs was obtained, with each epoch corresponding to a single packet index (the transmit duration corresponding

[1]We believe that the system's accuracy could be improved by using more receivers. However, for proof-of-concept demonstrations reported in this paper, two receivers suffice.

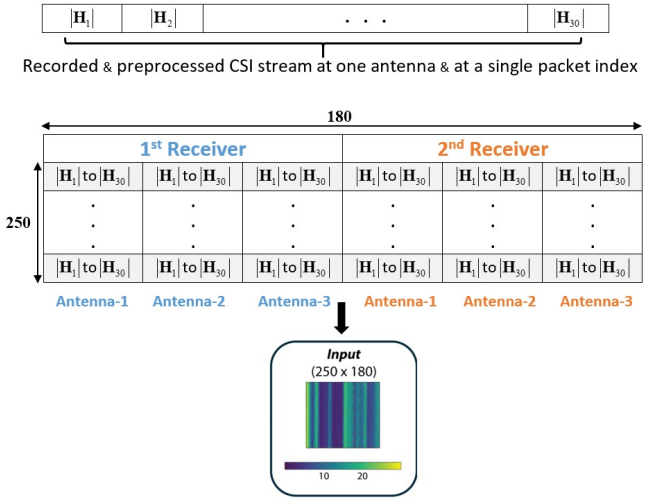

Fig. 2. Format of concatenated CSI data.

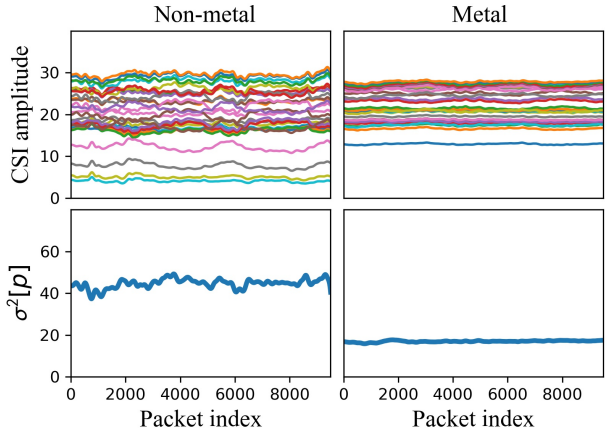

Fig. 3. Effect of metal on CSI amplitude and inter-carrier variance. The figures on the top display the CSI amplitude on the 30 measured sub-carriers.

to each packet was 1 ms, so this corresponds to a recording window of five seconds). This truncated stream is then passed through a Gaussian moving average filter to remove high frequency noise. Next, we use a non-overlapping window of size 20 to average the adjacent CSI recordings, thereby reducing 5000 recordings down to only 250 for each CSI stream. Reduced dimensionality helps in compressing the data and reducing the computational load associated with subsequent classification stage. To use the full potential of antenna diversity and fine-grained resolution provided by CSI subcarriers, we concatenate CSI data from all antennas of the two receiving nodes as shown in Fig. 2. Finally, we obtain a CSI matrix of size 250 $\times$ 180 for each experiment where 250 corresponds to total number of CSI recordings and 180 corresponds to the subcarrier dimension (six antennas $\times$ 30 subcarriers). We use this matrix as an input for feature extraction as explained in Section III-C.

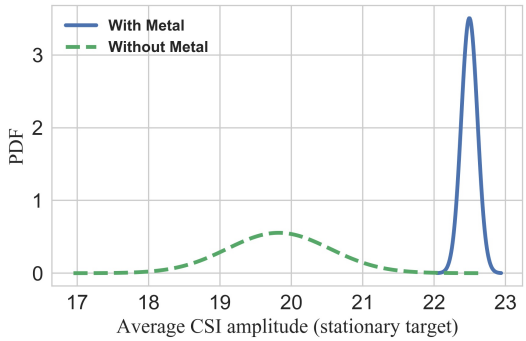

Fig. 4. Distribution of $\mu[p]$ - Static Case

III. Classification

In order to illustrate the effect of presence of metal in the illumination area, we first performed experiments with a stationary human target. For this case, we were able to clearly identify features in the received CSI stream that can draw a distinction between the presence and absence of metal. Next, we performed experiments with the target in motion. Since identification of differentiable shallow features in this case appears harder, we utilize a deep CNN for classification purposes. In the following, we first present our preliminary results with static subjects that provide useful insights into the effect of metal on radio signals. Next, we describe the challenges associated with a target in motion followed by a description of the deep CNN used for classification.

A. Static Target

For illustration purposes, we provide in Fig. 3 a sample of a single-antenna CSI stream for the two classes. The figures show a clear visual distinction between the two cases. In order to identify quantitative features for classification, we investigate the following two.

- **Average CSI amplitude:**

$$\mu[p] = \frac{1}{M}\sum_{i=1}^{M}|H_i[p]|. \tag{3}$$

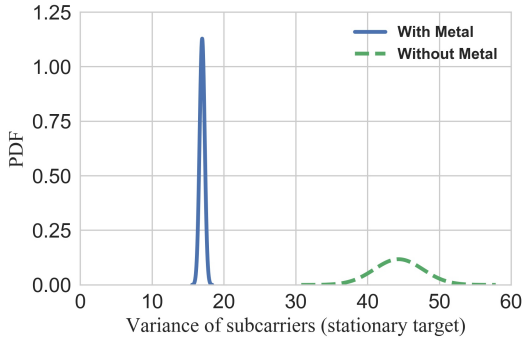

Fig. 5. Distribution of $\sigma^2[p]$ - Static Case

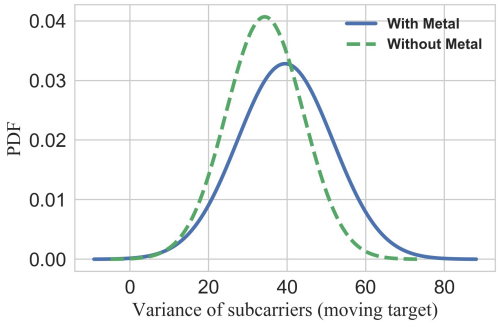

Fig. 6. PDF of $\sigma^2[p]$ - Target in Motion

- **Inter-carrier variance:**

$$\sigma^2[p] = \frac{1}{M-1}\sum_{i=1}^{M}\left[|H_i[p]| - \mu[p]\right]^2, \qquad (4)$$

where p indicates packet index, M total number of subcarriers and $|H_i[p]|$ is the CSI magnitude for i-th subcarrier at packet index p. Fig. 3 also indicates $\sigma^2[p]$ which is clearly distinguishable between metal and non-metal cases. To elucidate the distribution of these features, we plot in Figs. 4–5 the probability density function (PDF) associated with these features after fitting a normal curve to their histograms obtained from a total of 10,0000 measurements. While average CSI amplitude appears to be a reasonable measure, the inter-carrier variance $\sigma^2[p]$ is much more promising[2]. From Fig. 3, we note that $\sigma^2[p]$ in the presence of metal is smaller as compared to the one in its absence. A possible reason behind this is that a metal surface acts as a perfect reflector for radio frequency energy which makes reflections less diffusive. This is opposed to the absence of metal where the reflections arrive from the more diffusive stationary human body.

B. Moving Target

Contrary to the static cases, target motion along a predefined trajectory also induces motion artifacts in received CSI. As a result, the previously investigated features $\mu[p]$ and $\sigma^2[p]$ no longer remain reliable features. For instance, the fitted normal PDF associated with $\sigma^2[p]$ in Fig. 6 clearly shows a significant overlap between both classes, and hence may not serve as a reliable measure for classification when the target is in motion. Instead of manually identifying a better set of features, we resort to utilizing a CNN for recognizing the hidden patterns induced in CSI due to the presence of metallic objects.

C. Deep CNN

Our deep CNN architecture consist of multiple layers: input layer, hidden layer(s) and output layer. We have used one convolutional layer followed by one max pooling layer. In the classification stage, two fully connected hidden layers and a final output layer with *softmax* activation are used. When fed with the input data, the architecture is able to discover intricate and disguised patterns in the data thus finding and evaluating distinct features to be used inside the classification stage. Fig. 7 indicates the complete signal processing chain along with the deep CNN architecture we use. The first layer of CNN is a 2D convolutional layer with input shape of 250×180 followed by a 2D max pooling layer. After that, the data was flattened, and two hidden layers were used with 200 and 100 nodes respectively finally followed by the output layer. The parameters were modified such that training a model did not take exorbitant amounts of time. The details of the model are shown in Fig. 8.

[2]Although the PDFs have been depicted for an illustrative example, we point out that similar trend was observed on the remaining data sets as well.

IV. Experimental Results and Discussion

A. Experimental Setup

We prototyped our system using three Intel NUC (D54250WKH) boards equipped with Intel 5300 WiFi radios; the experimental setup is depicted in Fig. 9. One board acts as a transmitter and other two serve as receivers that are placed at 45° on either side of transmitting node. WiFi radio of the transmitting node is connected to a pyramidal horn antenna having ∼9dBi gain and 60° Half Power BeamWidth. On the other hand, each receiving node is connected to three omnidirectional antennas. To avoid interference related issues, we use 5 GHz frequency band because it is relatively less congested as compared to the crowded 2.4 GHz band. Channel 36 with 5.18 GHz center frequency having a bandwidth of 20 MHz is selected for CSI acquisition.

Experiments were conducted in an indoor environment that was effectively a hall of dimensions 42 ft × 39 ft. Receiver nodes are placed approximately 11.5 ft from the transmitter node. The duration of each experiment was set to around 10 seconds which involves a human subject approaching the transmitter node from a fixed position and stopping at another pre-defined position close to the transmitter. The distance between these two points was approximately 17 ft. We performed two types of experiments. In the first case, subjects approach the transmitter node without holding any metallic object, and in the second case, they carry a metallic aluminum sheet of dimensions 1 ft × 1 ft. We collected the data over multiple days with little environmental variation. Four people having different heights and body masses volunteered for our experiments. Multiple targets also help in accounting for different walking patterns, adding to the robustness of the system. In our setup, the transmitter is configured to send 802.11n compliant WiFi packets with 1 ms inter-packet delay. Packets are received at receiving nodes simultaneously after bouncing off the moving subject. At the receiver nodes, CSI is estimated and extracted for preprocessing.

B. Results and Evaluation

In total, we conducted 459 experiments with almost no differences in experimental setup for four people with and without metal sheet. The walking pace and angles for all subjects were kept almost the same with natural variations

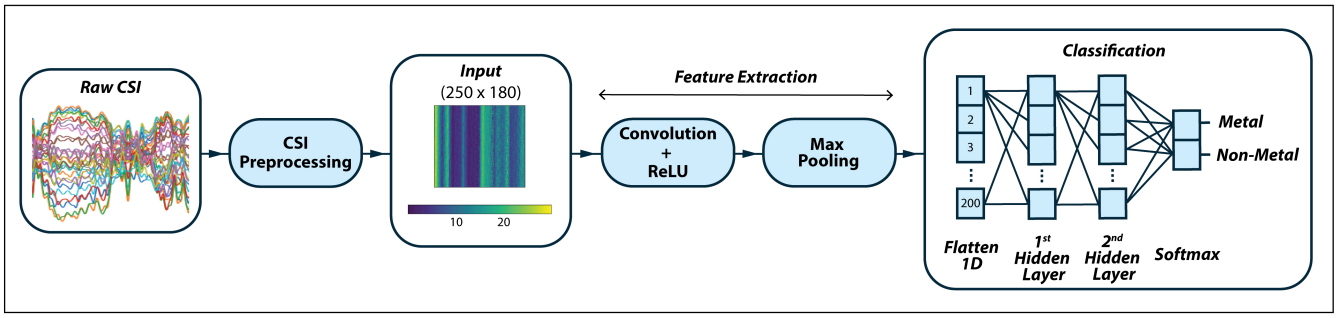

Fig. 7. CSI processing and classification chain.

Input Layer	(250 x 180) 2D Matrix
2D Convolution	Filters = 8, Kernel size = {2, 2}, Activation = 'ReLU'
2D Max Pooling	Pool size = {2, 2}
1st Hidden Layer	Nodes = 200, Activation = 'ReLU' with batch norm.
2nd Hidden Layer	Nodes = 100, Activation = 'ReLU', with batch norm.
Output Layer	Nodes = 2 (one-hot-encoding) Activation = 'Softmax'
Compiler	Optimizer = 'Nadam', Loss = MSE

Fig. 8. CNN model description.

only. The CSI data collected in these experiments were pre-processed and passed to CNN architecture for classification, with both the preprocessing and classification taking less than three seconds on the Intel NUC boards. The CNN model was trained and tested with 10-fold cross validation with around 500 epochs for convergence. As it is clear from Fig. 10 and Fig. 11, the validation accuracy and loss stabilized before 150 epochs. Fig. 12 shows the overall classification results producing an average testing accuracy of 86.44%.

C. Discussion

Experimental results presented in the previous sub-section show a great potential of using the proposed metal detection framework based on WiFi radios. An accuracy of 86.44% is achieved which further might be improved by designing a more robust classification stage. However, in all the experiments that we conducted, we have not checked the robustness of the system against certain parameters. As an example, all the experiments have been conducted with a single metal sheet. Also, during each experiment, there was only one target human either static or in motion. The system still needs to be tested

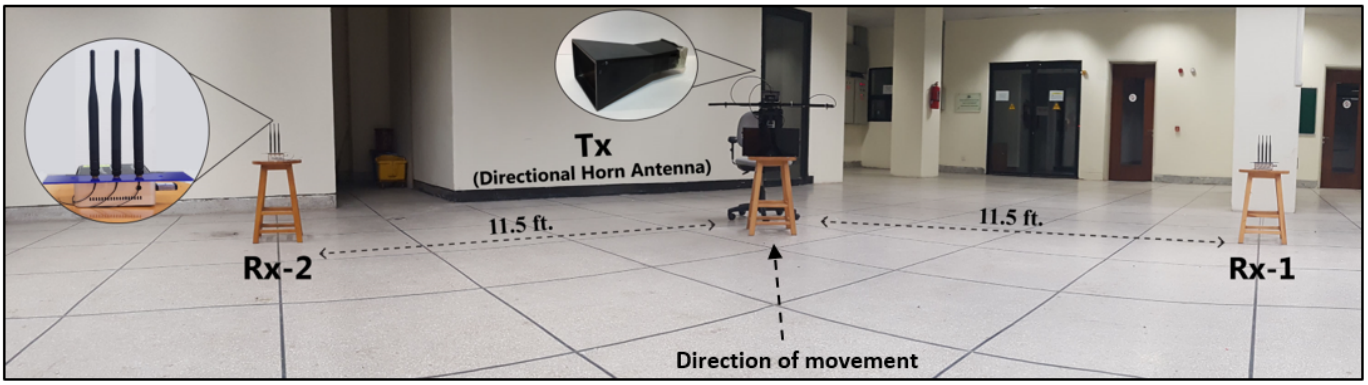

Fig. 9. The experimental setup.

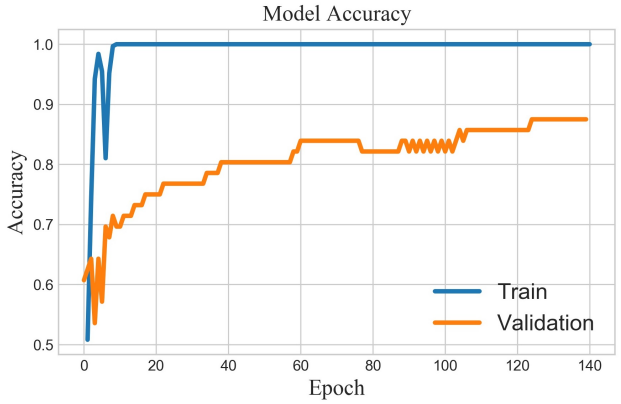

Fig. 10. CNN model accuracy probability.

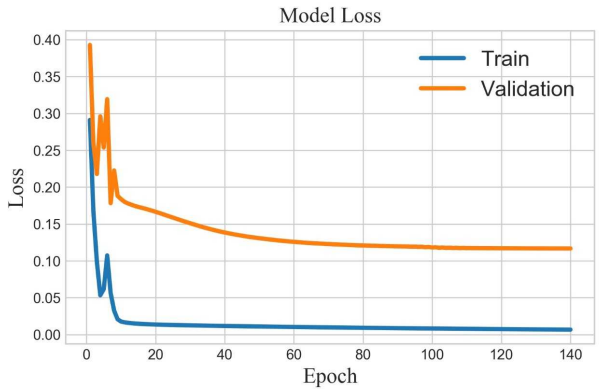

Fig. 11. CNN model loss probability.

and validated against such variations and uncertainties before a working deployable prototype is ready. Nevertheless, the preliminary results reported above point to the promise of using WiFi radios for non-obtrusive metal detection systems.

V. Conclusion

We have explored the use of commodity WiFi radios for developing a non-obtrusive system for concealed metallic object detection. By collecting data in an experimental setup where the subjects were asked to move through the setup with a concealed metallic object, we have demonstrated the effectiveness of the framework with a deep CNN classifier achieving an average accuracy of 86.44%. The robustness of the proposed system has been increased by deploying a number of receivers which simultaneously collect the reflected energy from the metallic object. Compared with previous systems, WiFi based metallic object detection systems, as proposed in this paper, have the potential to significantly increase the coverage area without requiring subjects to pass through a narrowly localized path. In the future, work will be extended to include detection of metallic objects carried by multiple persons along with more elaborate testing and experimental setup.

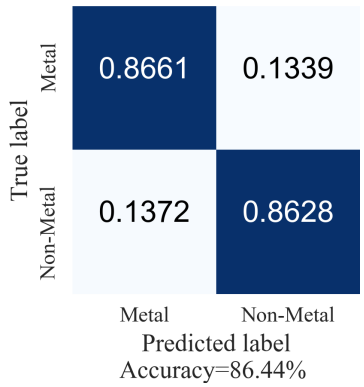

Fig. 12. Confusion matrix for the classification results probability.

References

[1] H. Frigui and P. Gader, "Detection and discrimination of land mines in ground-penetrating radar based on edge histogram descriptors and a possibilistic k-nearest neighbor classifier," *IEEE Transactions on Fuzzy Systems*, vol. 17, no. 1, pp. 185–199, 2009.

[2] R. P. Haff and N. Toyofuku, "X-ray detection of defects and contaminants in the food industry," *Sensing and Instrumentation for Food Quality and Safety*, vol. 2, no. 4, pp. 262–273, 2008.

[3] H. Ohanian and J. Markert, *Physics for Engineers and Scientist*. Norton & Company Inc., 2007.

[4] H.-M. Chen, S. Lee, R. M. Rao, M. A. Slamani, and P. K. Varshney, "Imaging for concealed weapon detection: a tutorial overview of development in imaging sensors and processing," *IEEE Signal Processing Magazine*, vol. 22, no. 2, pp. 52–61, March 2005.

[5] C. Liu, M.-H. Yang, and X.-W. Sun, "Towards robust human millimeter wave imaging inspection system in real time with deep learning," *Progress In Electromagnetics Research*, vol. 161, pp. 87–100, 2018.

[6] A. Elboushi and A. Sebak, "Mmw sensor for hidden targets detection and warning based on reflection/scattering approach," *IEEE Transactions on Antennas and Propagation*, vol. 62, no. 9, pp. 4890–4894, 2014.

[7] K. Wu, "Wi-metal: Detecting metal by using wireless networks," in *Communications (ICC), 2016 IEEE International Conference on*. IEEE, 2016, pp. 1–6.

[8] K. Wu, J. Xiao, Y. Yi, M. Gao, and L. M. Ni, "Fila: Fine-grained indoor localization," in *INFOCOM, 2012 Proceedings IEEE*. IEEE, 2012, pp. 2210–2218.

[9] D. Halperin, W. Hu, A. Sheth, and D. Wetherall, "Predictable 802.11 packet delivery from wireless channel measurements," in *ACM SIGCOMM Computer Communication Review*, vol. 40, no. 4. ACM, 2010, pp. 159–170.

[10] F. Xiao, J. Chen, X. H. Xie, L. Gui, J. L. Sun, and W. none Ruchuan, "Seare: A system for exercise activity recognition and quality evaluation based on green sensing," *IEEE Transactions on Emerging Topics in Computing*, 2018.

[11] X. Wang, C. Yang, and S. Mao, "Phasebeat: Exploiting csi phase data for vital sign monitoring with commodity WiFi devices," in *Distributed Computing Systems (ICDCS), 2017 IEEE 37th International Conference on*. IEEE, 2017, pp. 1230–1239.

[12] J. Shang and J. Wu, "A robust sign language recognition system with multiple WiFi devices," in *Proceedings of the Workshop on Mobility in the Evolving Internet Architecture*. ACM, 2017, pp. 19–24.

[13] K. Ali, A. X. Liu, W. Wang, and M. Shahzad, "Keystroke recognition using WiFi signals," in *Proceedings of the 21st Annual International Conference on Mobile Computing and Networking*. ACM, 2015, pp. 90–102.

[14] W. Wang, A. X. Liu, and M. Shahzad, "Gait recognition using WiFi signals," in *Proceedings of the 2016 ACM International Joint Conference on Pervasive and Ubiquitous Computing*. ACM, 2016, pp. 363–373.

[15] J. Lv, D. Man, W. Yang, X. Du, and M. Yu, "Robust WLAN-based indoor intrusion detection using PHY layer information," *IEEE Access*, 2017.

[16] J. Lv, W. Yang, and D. Man, "Device-free passive identity identification via WiFi signals," *Sensors*, vol. 17, no. 11, p. 2520, 2017.